

Analytical description of STED microscopy performance

Marcel Leutenegger,* Christian Eggeling, Stefan W. Hell

Department of NanoBiophotonics, Max Planck Institute for Biophysical Chemistry, Am Fassberg 11, 37077 Göttingen, Germany

*marcel.leutenegger@a3.epfl.ch

Stimulated emission depletion (STED) resolves fluorescent features that are closer than the far-field optical diffraction limit by applying a spatially modulated light field keeping all but one of these features dark consecutively. For estimating the efficiency of transient fluorophore darkening, we developed analytical equations considering the spatio-temporal intensity profile of the STED beam. These equations provide a quick analysis and optimization of the resolution and contrast to be gained under various conditions, such as continuous wave or pulsed STED beams having different pulse durations. Particular emphasis is placed on fluorescence fluctuation methods such as correlation spectroscopy (FCS) using STED.

©2010 Optical Society of America

OCIS codes: (050.1940) Diffraction; (180.2520) Fluorescence microscopy; (260.2510) Fluorescence.

References and links

1. S. W. Hell, and J. Wichmann, "Breaking the diffraction resolution limit by stimulated emission: stimulated-emission-depletion fluorescence microscopy," *Opt. Lett.* **19**(11), 780–782 (1994).
2. T. A. Klar, S. Jakobs, M. Dyba, A. Egner, and S. W. Hell, "Fluorescence microscopy with diffraction resolution barrier broken by stimulated emission," *Proc. Natl. Acad. Sci. U.S.A.* **97**(15), 8206–8210 (2000).
3. S. W. Hell, "Far-field optical nanoscopy," *Science* **316**(5828), 1153–1158 (2007).
4. A. Thomas, *Progress in Stimulated Emission Depletion Microscopy* (Shaker, Aachen 2001); Ph.D. thesis, Heidelberg (2001).
5. S. W. Hell, "Increasing the Resolution of Far-Field Fluorescence Microscopy by Point-Spread-Function Engineering," in *Topics In Fluorescence Spectroscopy 5: Nonlinear and Two-Photon-Induced Fluorescence*, J. Lakowicz, ed. (Plenum Press, New York, 1997).
6. B. Harke, J. Keller, C. K. Ullal, V. Westphal, A. Schönle, and S. W. Hell, "Resolution scaling in STED microscopy," *Opt. Express* **16**(6), 4154–4162 (2008).
7. The actual number of de-excitation events is limited by the number of excitations per pulse.
8. C. Ringemann, B. Harke, C. von Middendorff, R. Medda, A. Honigmann, R. Wagner, M. Leutenegger, A. Schönle, S. W. Hell, and C. Eggeling, "Exploring single-molecule dynamics with fluorescence nanoscopy," *N. J. Phys.* **11**(10), 103054 (2009).
9. V. Westphal, and S. W. Hell, "Nanoscale resolution in the focal plane of an optical microscope," *Phys. Rev. Lett.* **94**(14), 143903 (2005).
10. V. Westphal, C. M. Blanca, M. Dyba, L. Kastrop, and S. W. Hell, "Laser-diode-stimulated emission depletion microscopy," *Appl. Phys. Lett.* **82**(18), 3125–3127 (2003).
11. M. Dyba, and S. W. Hell, "Photostability of a fluorescent marker under pulsed excited-state depletion through stimulated emission," *Appl. Opt.* **42**(25), 5123–5129 (2003).
12. C. Eggeling, J. Widengren, R. Rigler, and C. A. M. Seidel, "Photobleaching of fluorescent dyes under conditions used for single-molecule detection: Evidence of two-step photolysis," *Anal. Chem.* **70**(13), 2651–2659 (1998).
13. W. Denk, J. H. Strickler, and W. W. Webb, "Two-photon laser scanning fluorescence microscopy," *Science* **248**(4951), 73–76 (1990).
14. K. I. Willig, J. Keller, M. Bossi, and S. W. Hell, "STED microscopy resolves nanoparticle assemblies," *N. J. Phys.* **8**(6), 106 (2006).
15. M. Leutenegger, R. Rao, R. A. Leitgeb, and T. Lasser, "Fast focus field calculations," *Opt. Express* **14**(23), 11277–11291 (2006).
16. M. Leutenegger, and T. Lasser, "Detection efficiency in total internal reflection fluorescence microscopy," *Opt. Express* **16**(12), 8519–8531 (2008).
17. K. I. Willig, B. Harke, R. Medda, and S. W. Hell, "STED microscopy with continuous wave beams," *Nat. Methods* **4**(11), 915–918 (2007).
18. S. W. Hell, "Toward fluorescence nanoscopy," *Nat. Biotechnol.* **21**(11), 1347–1355 (2003).

19. X. Hao, C. Kuang, T. Wang, and X. Liu, "Effects of polarization on the de-excitation dark focal spot in STED microscopy," *J. Opt.* **12**(11), 115707 (2010).
20. D. Magde, E. Elson, and W. Webb, "Thermodynamic fluctuations in a reacting system - measurement by fluorescence correlation spectroscopy," *Phys. Rev. Lett.* **29**(11), 705–708 (1972).
21. R. Rigler, and E. S. Elson, *Fluorescence Correlation Spectroscopy: Theory and Applications*, Springer Ser. Chem. Phys. **65**, Berlin Heidelberg, Germany (2001).
22. L. Kastrop, H. Blom, C. Eggeling, and S. W. Hell, "Fluorescence fluctuation spectroscopy in subdiffraction focal volumes," *Phys. Rev. Lett.* **94**(17), 178104 (2005).
23. D. E. Koppel, "Statistical Accuracy in Fluorescence Correlation Spectroscopy," *Phys. Rev. A* **10**(6), 1938–1945 (1974).
24. In case of a long-lived excited state, i.e. ≈ 12 ns in a nano-diamond nitrogen vacancy center [25], the required CW power is only about twice the average power for pulsed operation.
25. K. Y. Han, K. I. Willig, E. Rittweger, F. Jelezko, C. Eggeling, and S. W. Hell, "Three-dimensional stimulated emission depletion microscopy of nitrogen-vacancy centers in diamond using continuous-wave light," *Nano Lett.* **9**(9), 3323–3329 (2009).
26. E. Auksoorius, B. R. Boruah, C. Dunsby, P. M. P. Lanigan, G. Kennedy, M. A. A. Neil, and P. M. W. French, "Stimulated emission depletion microscopy with a supercontinuum source and fluorescence lifetime imaging," *Opt. Lett.* **33**(2), 113–115 (2008).

1. Introduction

Stimulated emission depletion (STED) overcomes the diffraction limit in fluorescence microscopy by ensuring that a (large) part of fluorophores in the diffraction-limited focal region is non-fluorescent (dark) for a brief period of time in which the remaining fluorophores are detected. As a result, a subset of fluorescent (bright) fluorophores is separated from a subset of dark neighbors within the diffraction region. Transient fluorescence deactivation is attained by a beam of light, called the STED beam, inducing stimulated emission from the fluorescent state of the dye [1–3]. Fluorophores that are exposed to an intensity I_{STED} of the STED beam that is well beyond a threshold I_s (at which the rate of stimulated emission equals the spontaneous decay) spend virtually all time in the ground state even when illuminated by excitation light; their capability to emit fluorescence is 'switched off'.

In the focal plane of a typical STED microscope an excitation light spot is overlaid with a STED light spot featuring a central intensity minimum ("zero"). In regions with high STED intensity I_{STED} the spontaneous decay of fluorophores is largely suppressed, but this is clearly not the case for those fluorophores residing at or close to the central minimum. The more intense the STED beam, the narrower the region becomes in which the fluorophores are allowed to emit. For most fluorophores the lifetime of the fluorescent state is in the order of nanoseconds and the cross section for stimulated emission σ_{STED} is about 10^{-17} – 10^{-16} cm². Hence a STED beam providing a time-averaged focal intensity $\langle I_{\text{STED}} \rangle \gg I_s \sim 5$ MW/cm² turns the fluorophores off even when they are flooded by excitation photons.

To keep the fluorophores dark using a moderate average laser power, most STED microscopes ('nanoscopes') employ a train of light pulses for both excitation and STED [1–3]. Numerical calculations of the STED efficiency have been performed elsewhere [1,2,4,5]; in the following, we will show how to optimize the performance of STED microscopy by tuning the pulse width of the STED beam. For this purpose, we calculate the fluorescence deactivation ('off-switching') efficiency by using approximations suitable for obtaining an analytical expression for the STED nanoscopy performance.

2. STED nanoscopy

STED efficiency

Figure 1 shows the Jablonski diagram of a typical organic fluorophore with the electronic ground singlet state S_0 , the electronic excited singlet state S_1 , the lowest triplet or other dark state T_1 , and vibrational sub-levels as well as the most relevant transitions between these states. After excitation from S_0 and vibrational relaxation, the fluorophore is found in the base level of the excited state S_1 , from where it spontaneously decays to S_0 or crosses to T_1 . If spontaneous decay takes place, a photon is emitted with a fluorescence quantum yield $q_f \leq 1$. On the other hand, the excited fluorophore can be sent down to a higher vibrational sub-level

S_0^* with a red-shifted light field inducing stimulated emission. If the stimulated emission rate is larger than the spontaneous decay, the fluorophore remains dark even under excitation irradiation; the residence in the excited state S_1 is essentially disallowed by the presence of the STED beam. Interruption of the STED beam turns the dye on instantly, because S_1 is allowed again. Keeping alternating features dark for a brief period of time enables the separation of features that are mutually closer than the diffraction limit. It is essential to realize that in the concept of STED microscopy, the sole purpose of the STED beam is to ensure that not all but just one of the features located within the diffraction region emits signal.

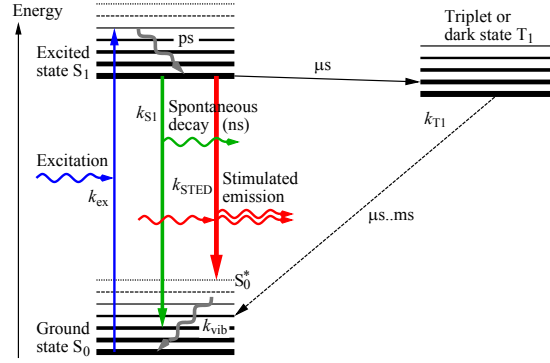


Fig. 1. Simplified Jablonski diagram with electronic and vibrational energy levels of a typical fluorophore.

For estimating the fluorescence ability of a fluorophore under STED, we assume that the fluorophore is initially in S_1 due to a short excitation pulse. Furthermore, we assume a rectangular STED pulse lasting for τ_{STED} , and a stimulated emission rate $k_{\text{STED}} = \zeta k_{S_1}$, with k_{S_1} denoting the spontaneous decay rate and $\zeta = I_{\text{STED}} / I_s$ being the saturation factor. ζ scales with the ratio of the pulse intensity I_{STED} of the STED light and the saturation (threshold) intensity I_s [6]. The saturation intensity here defines the STED intensity at which the rate $k_{\text{STED}} = \sigma_{\text{STED}} \Phi_{\text{STED}}$ of stimulated emission equals the spontaneous decay rate k_{S_1} (i.e., $\zeta = 1$). We define $\Phi_{\text{STED}} = I_{\text{STED}} \lambda_{\text{STED}} / (hc)$ as the photon flux, λ_{STED} is the STED wavelength in free space and $hc = 1.99 \cdot 10^{-25} \text{ Jm}$. Consequently, $I_s = k_{S_1} hc / (\lambda_{\text{STED}} \sigma_{\text{STED}})$ is a molecule-specific constant given by the cross section σ_{STED} of stimulated emission and k_{S_1} . During the STED pulse, i.e. for $0 < t < \tau_{\text{STED}}$, the relevant rate equations for the populations P_{S_1} of S_1 and $P_{S_0}^*$ of S_0^* , respectively, are

$$\begin{aligned} \frac{\partial}{\partial t} P_{S_1} &= -k_{S_1} P_{S_1} - k_{\text{STED}} (P_{S_1} - P_{S_0}^*) \\ \frac{\partial}{\partial t} P_{S_0}^* &= -k_{\text{vib}} P_{S_0}^* + k_{\text{STED}} (P_{S_1} - P_{S_0}^*) \end{aligned} \quad (1)$$

where k_{vib} is the vibrational relaxation rate of S_0^* to S_0 . We normalize the populations to one molecule, i.e. $P_{S_1}(0) = 1$; all other states are initially unpopulated. Because $k_{\text{vib}} \gg k_{S_1}$ and as long as $\tau_{\text{STED}} \gg 1/k_{\text{vib}}$, the equilibration of the population $P_{S_0}^*$ is fast, such that the excited state population can be well approximated by $P_{S_1}(0 < t < \tau_{\text{STED}}) \approx \exp(-k_{S_1} t (1 + \gamma))$, where $\gamma = \zeta k_{\text{vib}} / (\zeta k_{S_1} + k_{\text{vib}})$ is the effective saturation factor that also accounts for the generally undesired excitation from S_0^* to S_1 by the STED beam itself. Thereafter, the excited state population spontaneously decays at a rate k_{S_1} and is simply given by

$P_{S_1}(\tau_{\text{STED}} < t < T) \approx \exp(-k_{S_1}(\gamma\tau_{\text{STED}} + t))$, where T is the period between two STED pulse peaks in a pulse train, i.e. the inverse of the pulse repetition rate. The fluorescence probability F per molecule is then given by

$$F(\gamma) = q_{\text{fl}} k_{S_1} \int_0^T P_{S_1}(t) dt = q_{\text{fl}} \left(\frac{1 + \gamma \exp(-k_{S_1} \tau_{\text{STED}} (1 + \gamma))}{1 + \gamma} - \exp(-k_{S_1} (\gamma \tau_{\text{STED}} + T)) \right). \quad (2)$$

The probability of spontaneous decay η_{ps} is now obtained as $F(\gamma)/F(0)$, which equals the fraction to which the fluorescence is suppressed by the STED pulse of intensity I_{STED} (which is proportional to ζ and γ), and where $F(0) = q_{\text{fl}}(1 - \exp(-k_{S_1}T))$ is the fluorescence probability of the undisturbed molecule.

$$\eta_{\text{ps}} = \left(\frac{1 + \gamma \exp(-k_{S_1} \tau_{\text{STED}} (1 + \gamma))}{1 + \gamma} - \exp(-k_{S_1} (\gamma \tau_{\text{STED}} + T)) \right) (1 - \exp(-k_{S_1}T))^{-1} \quad (3)$$

This is the main equation describing STED analytically.

Here, $k_{S_1} \tau_{\text{STED}}$ and $\gamma k_{S_1} \tau_{\text{STED}} \approx k_{\text{STED}} \tau_{\text{STED}} = \zeta k_{S_1} \tau_{\text{STED}} = I_{\text{STED}} \sigma_{\text{STED}} \tau_{\text{STED}}$ characterize the average number of spontaneous and the average number of possible stimulated de-excitation events during the STED pulse τ_{STED} , respectively [7]. $k_{\text{STED}} \tau_{\text{STED}}$ is a measure of the strength of the applied STED irradiation. For a constant pulse repetition rate $1/T$, it scales linearly with the average STED power $\langle P_{\text{STED}} \rangle$.

If the period T is long compared to the excited state lifetime, $k_{S_1}T$ is large and Eq. (3) simplifies to the first term, i.e.

$$\eta_{\text{ps}} \approx \frac{1 + \gamma \exp(-k_{S_1} \tau_{\text{STED}} (1 + \gamma))}{1 + \gamma}. \quad (4)$$

For large $k_{S_1} \tau_{\text{STED}} (1 + \gamma)$, Eq. (4) becomes then

$$\eta_{\text{ps}} \approx 1 / (1 + \gamma). \quad (5)$$

This is the case for long STED pulses, i.e. for the case of applying pulsed excitation in conjunction with continuous wave (CW) STED ($\tau_{\text{STED}} = T$). The equation also holds for large k_{S_1} , i.e. for fluorophores with short fluorescence lifetimes, in which case I_s is large and the I_{STED} necessary to achieve a certain fluorescence inhibition becomes very large as well. Likewise Eq. (5) also applies if large I_{STED} , i.e. large ζ and γ are used. This condition also defines the maximum achievable fluorescence inhibition $\eta_{\text{ps}}(k_{\text{STED}} \rightarrow \infty) = 1 / (1 + k_{\text{vib}} / k_{S_1})$, which is determined by the finite vibrational relaxation rate k_{vib} . For typical fluorophores and measurement conditions, the ratio $k_{\text{vib}}/k_{S_1} \sim 10^3 - 10^4$ ($k_{S_1} \sim 1/\text{ns}$ compared to $k_{\text{vib}} > 1/\text{ps}$), hence $\eta_{\text{ps}} < 1\%$ approaches almost complete fluorescence suppression. An infinite relaxation rate results in $\eta_{\text{ps}} \approx 1 / (1 + \zeta) = 1 / (1 + I_{\text{STED}} / I_s) \rightarrow 0$ for $I_{\text{STED}} \rightarrow \infty$. In most experiments however, $\eta_{\text{ps}}(I_{\text{STED}} \rightarrow \infty) > 0$ because of a small though non-zero probability of $S_0 \rightarrow S_1$ excitation by the STED light.

Equation (3) is applicable for pulsed excitation; STED can be either pulsed or CW. In case of CW excitation and CW STED, the ongoing excitation continuously works against the inhibition of the fluorescent state occupation, i.e. against the off-switching of the fluorophore. Neglecting the triplet state, the probability of spontaneous decay η_{CW} writes as

$$\eta_{\text{CW}} \approx \frac{k_{\text{ex}} + k_{S_1}}{k_{\text{ex}} + (1 + \gamma)k_{S_1}}. \quad (6)$$

This is the main equation for CW STED, which derives from the ratio of the average time periods a fluorophore requires for a spontaneous decay from S_1 with and without STED.

Without STED, this is the time for a full excitation–de-excitation cycle $k_{\text{ex}}^{-1} + k_{\text{S}_1}^{-1}$. With STED, more excitations by a factor of γ are required, that is a time of $(1 + \gamma)k_{\text{ex}}^{-1} + k_{\text{S}_1}^{-1}$ per spontaneous decay. For low excitation avoiding saturation of the $S_0 \rightarrow S_1$ transition ($k_{\text{ex}} \ll k_{\text{S}_1}$), Eq. (6) simplifies to the expression of Eq. (5). In this case of CW STED the same fluorescence inhibition is achieved regardless of applying pulsed or CW excitation. More detailed calculations taking into account the pulse delay as well as the excitation power and triplet state dependent response are summarized in the annexes.

Previous work has given different descriptions of the fluorescence inhibition efficiency η_{ps} by STED [6]. Assuming $k_{\text{vib}} \rightarrow \infty$ and regarding only the residual fluorescence emitted *after* the STED pulse, η_{ps} was calculated from the single rate equation $\partial P_{\text{S}_1} / \partial t = -k_{\text{S}_1} P_{\text{S}_1} - k_{\text{STED}} P_{\text{S}_1}$ as the remaining population of S_1 after the pulse duration τ_{STED} .

$$\eta_{\text{ps}}^* = \exp(-k_{\text{S}_1} \tau_{\text{STED}} \gamma) = \exp(-\ln(2) I_{\text{STED}} / I_s^*) \quad (7)$$

The saturation intensity $I_s^* = \ln(2)hc / (\lambda_{\text{STED}} \sigma_{\text{STED}} \tau_{\text{STED}})$ had been introduced as the STED intensity to inhibit half of the S_1 population, i.e. half of the spontaneously emitted fluorescence ($\eta_{\text{ps}}^*(I_s^*) = 0.5$) after the STED pulse. Equation (3) differs mainly in the aspects that it accounts for k_{vib} and the pulse period T and that it includes the spontaneous fluorescence emitted during the STED pulse.

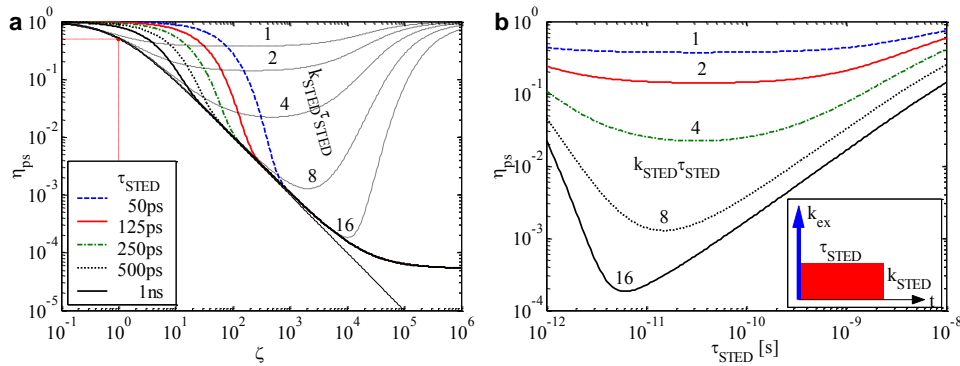


Fig. 2. Probability of spontaneous decay η_{ps} as a function of the saturation factor ζ and the pulse width τ_{STED} of the STED light (as labeled) for $k_{\text{S}_1} = 1/3.9\text{ns}$, $k_{\text{vib}} = 5/\text{ps}$ and $T = 1/80\text{MHz}$. (a) The thin line shows the lower limit achieved for CW STED and infinitely fast vibrational relaxation. Thin dashed lines show the dependence of η_{ps} on variable pulse lengths τ_{STED} for fixed numbers of potential de-excitations $k_{\text{STED}}\tau_{\text{STED}}$, i.e. for fixed average STED powers. (b) This dependence is shown as a function of τ_{STED} . The inset outlines the pulse scheme used in the calculations: a Dirac excitation pulse followed by a rectangular STED pulse.

Pulse length dependence

Figure 2 outlines the estimated STED performance, i.e. the probability of spontaneous decay η_{ps} versus ζ (i.e. pulse STED intensity) calculated for $k_{\text{S}_1} = 1/3.9\text{ns}$, $k_{\text{vib}} = 5/\text{ps}$ and 80MHz pulse rate. These values are taken from the organic dye Atto647N in a supported lipid bilayer [8] and a mode-locked Ti:Sapphire laser. In Fig. 2a, the thin line shows the lower limit $1/(1 + \zeta)$, which is achieved for pulsed excitation but continuous wave (CW) STED and infinite k_{vib} . The bold lines indicate the performance for pulsed STED (Eq. (3)) showing an ever more pronounced knee, the shorter the STED pulses become. This is because the STED intensity has to counterbalance the short excited state depletion time before the suppression becomes efficient. Regardless of the pulse width, the suppression efficiency saturates at a lower bound (here $\eta_{\text{ps}} \approx 5 \cdot 10^{-5}$) due to the vibrational relaxation rate k_{vib} , which sets the upper limit for the effective stimulated depopulation rate of S_1 (Eq. (5)). In addition, the thin dotted

lines of Fig. 2a and the lines of Fig. 2b trace η_{ps} versus ζ and τ_{STED} , respectively, for constant average STED powers that potentially stimulate the S_1 de-excitation $k_{STED}\tau_{STED} = \zeta k_{S1}\tau_{STED}$ equals 1–16 times per pulse.

Increasing ζ or τ_{STED} along the $k_{STED}\tau_{STED}$ isolines entails an according decrease of τ_{STED} and ζ , respectively. For very long pulses, i.e. small ζ , the suppression of the fluorescent state is quite inefficient because spontaneous emission is as fast or faster. For very short pulses on the other hand, i.e. large ζ , the suppression becomes inefficient again because of the limited S_1 de-excitation rate stemming from the finite vibrational relaxation rate k_{vib} . Figure 2 reveals that a pulse width of $\tau_{STED} \approx 20\text{--}30\text{ps}$ would exploit the available STED power maximally and would yield the steepest decrease of η_{ps} with increasing ζ . Both characteristics are preferable in STED imaging as outlined further on.

In many practical cases however, it turned out that a pulse width of $\tau_{STED} \approx 100\text{--}150\text{ps}$ leads to better results. The following reasons can be cited. Firstly, longer pulses leave more time for the excited molecules to rotate, which helps minimizing polarization effects [9]. Secondly, if pulsed diode lasers are used for excitation [10], the excitation pulse width of about 50–70ps and the synchronization jitter can be better countered with longer STED pulses. Thirdly, it has been shown that longer pulses are more advantageous with respect to photobleaching of the fluorophores [11], since these phenomena usually scale with higher orders of the intensity [12]. Strongly related with the previous argument is the fact that longer pulses disfavor multiphoton excitation processes, including plain multiphoton excitation of relaxed molecules from the ground state [13].

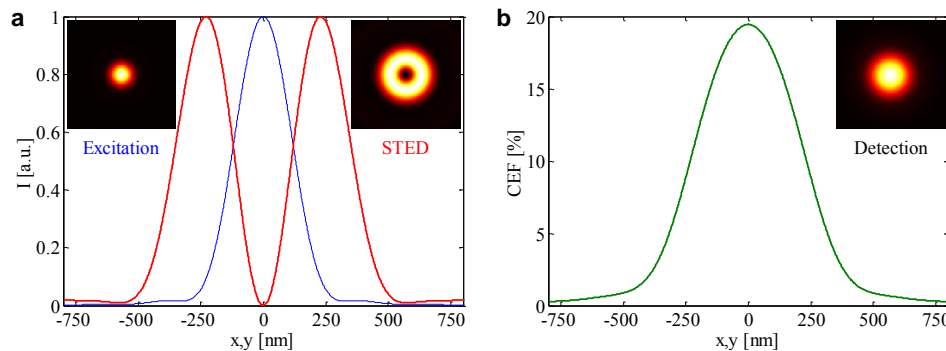


Fig. 3. Cross-sections through the foci of the excitation and the STED light spots (a) and of the fluorescence collection efficiency (b) used in the calculation examples. Insets show the spot profiles in the xy -planes.

Spatial resolution and STED imaging

In the focal plane of a typical STED microscope a diffraction-limited excitation light spot is overlaid with a STED light spot featuring a local intensity minimum at the center of the excitation spot. An example is the doughnut-shaped intensity pattern recalled in Fig. 3 [14]. Consequently, fluorescence is inhibited everywhere but at the focal center and the more intense the STED beam, the more fluorophores and fluorescent features are switched off by the STED light and the narrower the region becomes in which the fluorophores are allowed to fluoresce. Figure 4 exemplifies calculated cross-sections through effective STED point-spread-functions (PSF) of such a confocal epi-fluorescence microscope with an oil immersion objective of numerical aperture (NA) of 1.40 and a fluorescent dye with a lifetime of 3.9ns [15,16]. The effective STED PSF describes the region in which the dyes are allowed to emit and subsequently be registered by the detector. More precisely, it gives the normalized probability with which the fluorophore is able to contribute to the measured signal at a given location in the sample. The excitation wavelength λ_{ex} is 635nm and the STED wavelength λ_{STED} is 770nm. Both beams overfill the objective aperture and are circularly polarized. The STED beam passes through a 2π phase ramp (vortex plate) for creating a doughnut with a

central “zero”, i.e. a minimum with a relative intensity of ϵ times the intensity at the doughnut crest [6]. The detection pinhole has a projected diameter of 500nm in the sample space, i.e. $0.9 \times$ the Airy disc diameter. At low excitation intensity, the detected fluorescence brightness profile is the product of the excitation probability times the emission probability η times the detection efficiency.

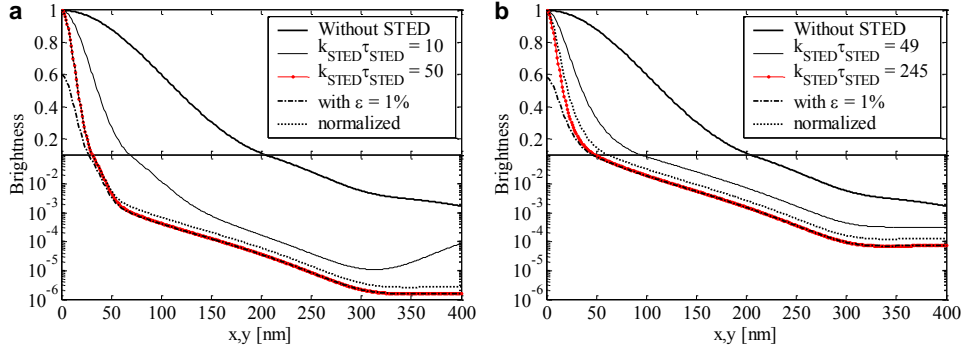


Fig. 4. Effective PSF of a STED nanoscope with (a) pulsed ($\tau_{\text{STED}} = 50\text{ps}$) and (b) CW STED ($\tau_{\text{STED}} = T = 12.5\text{ns}$): lateral cross-sections of the detected fluorescence brightness without STED (bold solid lines) and with average STED powers required for achieving FWHM diameters of 72nm (thin solid lines) and 33nm (pointed red lines). Dash-dotted lines show the profiles with an imperfect “zero” and dotted lines show them normalized again to their peak brightness. For values below 10% of the peak brightness, the logarithmic scale allows a better distinction of the differences.

Without STED, the detected fluorescence ($\lambda_{\text{fl}} = 670\text{nm}$) has a brightness profile with a full width at half-maximum (FWHM) diameter of 232nm. Applying STED pulses or CW STED irradiation, the FWHM diameter is narrowed with increasing STED power in all cases and follows a similar dependence regardless of the STED modality as summarized in Fig. 5.

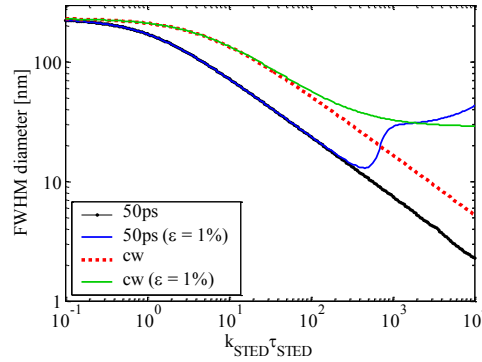


Fig. 5. FWHM diameters versus STED power. For $k_{\text{STED}}\tau_{\text{STED}} > 500$ in case of 50ps STED pulses with $\epsilon = 1\%$, the increase of the FWHM indicates loss of signal due to a too strong reduction of the central peak brightness versus the contributions from the focal periphery.

For obtaining the same FWHM diameter, the CW STED power has to be increased about five fold ($\sim 1.5k_{\text{S1}}T$) as compared to the average STED power in the pulsed case [17]. As predicted [18] and experimentally verified [9], the inverse of the FWHM diameters of the STED foci follow a square root law. In the pulsed mode, the FWHM is about $\text{FWHM}_0 / \sqrt{1 + k_{\text{STED}}\tau_{\text{STED}}}$ with the diffraction limited confocal $\text{FWHM}_0 \approx 0.52\lambda_{\text{ex}}/\text{NA}$ and where $k_{\text{STED}}\tau_{\text{STED}}$ is the number of potential stimulated emission events per molecule at the doughnut crest (if there were as many excitations). With 50ps long STED pulses and $k_{\text{STED}}\tau_{\text{STED}} = 50$ at the crest, a FWHM of about 33nm is reached in the outlined example. In the

vicinity of the “zero”, changing the pulse width τ_{STED} does not significantly alter the profile as shown by the CW PSF, where the STED “pulse width” equals the excitation pulse period $T = 12.5\text{ns}$.

In Fig. 4, the dash-dotted lines show the effect of an imperfect “zero” with a residual intensity amounting to $\varepsilon = 1\%$ of the crest intensity. In the outlined examples, a vortex plate is used for creating the doughnut, which is rather tolerant to many experimental imperfections such as astigmatic or spherical wave front aberrations or lateral misalignments. Using a vortex plate, an imperfect zero typically stems from wrongly polarized light (c.f. [19] for examples) and/or from asymmetric wave front aberrations. For instance, elliptically polarized light with an electric field varying by $\sim 20\%$ peak-to-peak results in $\varepsilon = 1\%$. In this case, the peak brightness drops significantly, in particular at high STED power, but the diameter is hardly affected for short STED pulses. However, with CW STED the resolution deteriorates (with respect to the case of $\varepsilon = 0$) to a value of FWHM = 43nm as shown by the normalized profiles. Note, that along with the reduction of the fluorescence at the central peak, suppression of fluorescence is not complete in the focal periphery. While the contribution of this peripheral fluorescence is in principle low, it is less for short STED pulses and for $\varepsilon = 0$, i.e. the effective STED PSF is sharper and offers a better contrast. The improved performance in the case of short STED pulses results from the steep dependence of η_{ps} with increasing ζ (Fig. 2).

3. STED nanoscopy for fluorescence fluctuation spectroscopy

So far, we measured the resolution by the FWHM of the central peak. Unfortunately, this measure may become inappropriate for very high resolution, i.e. small FWHM values. Because the emission of peripheral fluorophores cannot be suppressed completely, their contribution to the total signal becomes increasingly important in this case (Fig. 4). As long as STED nanoscopy is applied for imaging comparatively sparse features, the effective PSF in real space, respectively its optical transfer function (OTF) in Fourier space, can be usually exploited for reducing undesired image artifacts like blur or ghost images. Within the limits of the signal-to-noise ratio (SNR) of the image(s), image deconvolution allows improving the image quality by re-attributing faint peripheral signals to their original features. However, such image restoration methods are hardly (if ever) applicable for spectroscopic measurements, such as fluorescence correlation spectroscopy (FCS) [20,21] for instance, essentially because the fluorescence signal from randomly distributed and/or mobile fluorophores is collected and the spatial information (neighborhood) has to be ignored in favor of sufficient time resolution, i.e. the assumption of sparse and spatio-temporally resolved features fails. For example, previous STED-FCS measurements of fluorophores diffusing in open measurement volumes of nanoscale dimensions showed a decrease in signal-to-background ratio (SBR) with increasing resolution due to a growing contribution of peripheral fluorescence [8,22]. Besides increasing the noise in the FCS data, a poor SBR damps the correlation amplitude, impeding the determination of concentration and brightness values [23].

In order to quantify the performance of STED in FCS, we introduce a general measure based on the SBR within a homogeneous sample. Note that a spatially homogeneous sample represents a well-defined worst case, i.e. non-structured and hence non-resolvable case in imaging, whereas it is virtually the default case in FCS (when the random molecular trajectories are averaged over time). The SBR shall denote the contrast between the signals from the brightest focal region(s) compared to the background from the dimmer region(s), where we apply an arbitrary threshold to separate the bright from the dim region(s). For 50ps pulsed and CW STED irradiation, Fig. 6 exemplifies the SBR versus the radii of the bright signal area for a threshold set at 10% of the maximum fluorescence intensity in the focal center. Without STED, the signal area has a radius of about 203nm and nearly 90% of the detected fluorescence is emitted within this area (SBR ≈ 8.6). With increasing STED power, the SBR decreases along with the radius of the signal area.

The decrease of the SBR is much more pronounced for the CW than for the pulsed STED mode. With a perfect “zero” ($\varepsilon = 0$), the SBR remains >3 for signal area radii $>5\text{nm}$ in pulsed mode and 118nm with CW STED, respectively. This significant advantage of pulsed STED

was experimentally observed when comparing STED-FCS measurements in pulsed and CW STED mode [8]. With $\varepsilon = 1\%$ residual intensity in the “zero”, this radius increases sharply from 5nm to 30nm in the pulsed mode, because the bright central region is no longer able to surpass three-fold the background from the entire periphery. In this case, increasing the STED power further can even lead to a complete loss of signal, which is indicated by the return point on the curve in Fig. 6a, where the diameter increases because the first order side lobe (Airy ring) becomes part of the signal area. For the same imperfect “zero” in CW STED, the diameter hardly increases to about 119nm because the peripheral regions always contribute notable background (Fig. 4b).

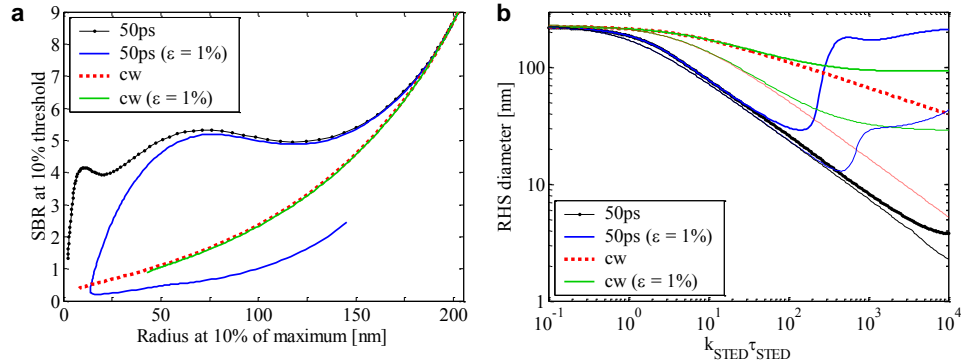


Fig. 6. (a) SBR at 10% of maximum threshold. (b) RHS diameters (thin lines: FWHM).

With the SBR set up here, an effective size of the STED focal region for FCS may be obtained as the area or volume of the brightest focal region(s). Analogous to the FWHM, requiring a SBR = 1 yields a region of half-signal (RHS) from where 50% of the detected signal originates. Figure 6b compares the FWHM diameter with the RHS diameter $2\sqrt{\text{RHS}/\pi}$, if the outlined system is used to investigate a two-dimensional sample, such as fluorophores diffusing in a membrane sheet in the focal plane. For low to medium STED power, the RHS diameter follows the FWHM with < 20% difference. If $k_{\text{STED}}\tau_{\text{STED}}$ increases beyond the maximum contrast between the “zero” and the crest region, the RHS diameter deviates and eventually grows again, which accounts for a too dim signal from the tiny effective STED PSF. For the outlined example, the minimal RHS diameters are about 4nm (50ps) and 29nm (50ps with $\varepsilon = 1\%$) at $k_{\text{STED}}\tau_{\text{STED}} \approx 10^4$ and 140, respectively.

As pointed out and demonstrated, STED does not require pulsed operation [17]. In the outlined case of a fluorophore with 3.9ns lifetime and a STED laser with 80MHz pulse rate, pulsed excitation but CW STED would just require about five times the average pulsed STED power in order to obtain equivalent FWHM diameters [24,25]. For FCS however, it became clear that the CW STED performs significantly worse because the fluorescence in the peripheral region is less efficiently suppressed. This is indicated by minimal CW RHS diameters of 40nm with perfect and 93nm with $\varepsilon = 1\%$ “zero”, respectively. With strong CW excitation, the situation may even become worse because fluorophores in the periphery cycle more often than those in the center (c.f. annexes).

4. Conclusions

In summary, we outlined a straightforward analytical model that allows a rather accurate estimation of the inhibition of spontaneous fluorescence by STED and the resulting brightness profiles in the effective STED PSF, i.e. in the region in which the fluorophore remains bright. This region scales down in diameter with a factor proportional to the square root of the number of stimulated emission events per molecule that are in principle possible (maximum statistical average) at the focal intensity maximum of the STED beam. We introduced a combined resolution and contrast measure, the region of half-signal (RHS), stating that the collected signal from within the tiny region in which the dye is allowed to fluoresce should

preferably be at least as large as all background contributions from elsewhere, in particular from the focal periphery. For nearly perfect “zeros”, the FWHM diameter continuously shrinks with increasing STED power, whereas the RHS diameter decreases only as long as the fluorophores in the active region generate enough signal to overcome the background from their neighbors. The achievable RHS diameters are smaller in the pulsed than in the CW STED mode, because the pulsed mode better suppresses the excited state in the focal periphery for a given number of stimulating photons.

However, it is worth noting that remedies can be found. If pulsed excitation is used, time-gated detection improves the performance if the early spontaneous emission of the fluorophore is discarded [26]. Likewise, it is important to understand that the outlined RHS ruler fully applies only to the most unfavorable case, i.e. a dense sample with many fluorophores in the focal periphery, each contributing. Whereas this assumption holds for most spectroscopic measurements such as FCS, which typically disregard spatial information in favor of time resolution, it represents a rare worst case in imaging, where the effective PSF (or the corresponding optical transfer function) can be fully exploited for improving the image based on the spatial information discriminating the neighboring features. In both cases, our simple model allows optimizing the experimental conditions for STED nanoscopy as well as taking into account the effective STED PSF for an improved analysis of the measurement data.

Annexes

The probability of spontaneous decay η is given by the ratio of the fluorescence $F(\gamma)$ under STED versus the fluorescence $F(0)$ without STED. The emission rate per fluorophore k_{fl} is the product of the fluorescence quantum yield q_{fl} and the rate of spontaneous decays k from the excited state S_1 : $F \propto k_{\text{fl}} = q_{\text{fl}}k$.

Pulsed excitation

The derivation of Eq. (3) and its simplifications are outlined in section 2 and summarized as case 2–4 in Table 1 (cumulative conditions). If the STED pulse follows the excitation pulse with a delay τ , $1 - \exp(-k_{S_1}\tau)$ spontaneous decays take place before the start of the STED pulse and only the remaining fraction $\exp(-k_{S_1}\tau)$ of molecules are affected (case 1).

Table 1. STED efficiency $\eta_{\text{ps}} = n_{S_1}(\gamma)/n_{S_1}(0)$ with instantaneous excitation and pulsed or continuous STED irradiation.

Case/conditions	Spontaneous decays within a pulse period T	
	$n_{S_1}(\gamma)$	$n_{S_1}(0)$
1: $\tau_{\text{ex}} \ll 1/k_{S_1}$	$1 - \exp(-k_{S_1}\tau) + \exp(-k_{S_1}\tau) \frac{1 + \gamma \exp(-k_{S_1}\tau_{\text{STED}}(1 + \gamma))}{1 + \gamma} - \exp(-k_{S_1}(\gamma\tau_{\text{STED}} + T))$	$1 - \exp(-k_{S_1}T)$
2: $\tau \rightarrow 0$	$\frac{1 + \gamma \exp(-k_{S_1}\tau_{\text{STED}}(1 + \gamma))}{1 + \gamma} - \exp(-k_{S_1}(\gamma\tau_{\text{STED}} + T))$	$1 - \exp(-k_{S_1}T)$
3: $k_{S_1}T \gg 1$	$\frac{1 + \gamma \exp(-k_{S_1}\tau_{\text{STED}}(1 + \gamma))}{1 + \gamma}$	1
4: $k_{\text{STED}}\tau_{\text{STED}} \gg 1$	$\frac{1}{1 + \gamma}$	1

As long as the fluorescence response follows the excitation intensity linearly, the fluorescence emission is proportional to the product of the excitation intensity and the spontaneous emission probability. However, for larger excitation intensities, the ground state

S_0 of the fluorophore becomes depopulated during the excitation pulse (saturated excitation) and/or because of triplet state accumulation. For the sake of simplicity, we keep assuming $\tau_{\text{ex}} \ll 1/k_{S_1}$ (instantaneous excitation) and assume in addition $k_{S_1} \gg k_{T_1}$ (slow triplet decay).

Let P_X^- be the population of the molecular state X just before the excitation pulse and P_X^+ just thereafter. Let n_{S_0} be the number of excitations from the ground state S_0 during the excitation pulse. The singlet state populations are then described by the following relations:

$$\begin{aligned} P_{S_0}^- &= 1 - P_{S_1}^- - P_{T_1}^- \\ P_{S_1}^+ &= P_{S_1}^- + n_{S_0} P_{S_0}^- \\ P_{S_1}^- &= \exp(-k_{S_1}(\gamma\tau_{\text{STED}} + T)) P_{S_1}^+ \end{aligned} \quad (8)$$

The triplet state T_1 is populated via intersystem crossing, whose number of transitions is the product of the intersystem crossing probability q_{isc} and the number n_{S_1} of spontaneous decays from S_1 . The triplet population relaxes then with the rate k_{T_1} to the ground state S_0 .

$$\begin{aligned} P_{T_1}^+ &\approx P_{T_1}^- + q_{\text{isc}} n_{S_1} P_{S_1}^+ \\ P_{T_1}^- &\approx \exp(-k_{T_1} T) P_{T_1}^+ \end{aligned} \quad (9)$$

At the dynamic equilibrium, Eq. (9) yields the triplet population $P_{T_1}^- \approx q_{\text{isc}} n_{S_1} P_{S_1}^+ / (\exp(k_{T_1} T) - 1)$ and insertion into Eq. (8) yields then a relation for the population of the excited singlet state S_1 .

$$P_{S_1}^+ = n_{S_0} + (1 - n_{S_0}) \exp(-k_{S_1}(\gamma\tau_{\text{STED}} + T)) P_{S_1}^+ - \frac{q_{\text{isc}} n_{S_1} n_{S_0} P_{S_1}^+}{\exp(k_{T_1} T) - 1} \quad (10)$$

Solving Eq. (10) for $P_{S_1}^+$ and noting that the rate of spontaneous decays k_{ps} is given by $n_{S_1} P_{S_1}^+ / T$, we finally obtain

$$k_{\text{ps}} = \frac{n_{S_1} n_{S_0}}{T} \left(1 - (1 - n_{S_0}) \exp(-k_{S_1}(\gamma\tau_{\text{STED}} + T)) + \frac{q_{\text{isc}} n_{S_1} n_{S_0}}{\exp(k_{T_1} T) - 1} \right)^{-1}. \quad (11)$$

Equation (11) includes the effect of the triplet state accumulation, which is most pronounced at the local “zero” of the STED beam, where the spontaneous decays are most frequent. Therefore, if a fluorophore shows a significant triplet state population, the accumulation in the dark triplet state will lead to a significant reduction of the fluorophores brightness in the vicinity of the “zero”, much as if there would be some residual STED light.

In addition to the triplet state accumulation, saturated excitation occurs at higher excitation rates k_{ex} because of the depopulation of the ground state S_0 during the excitation pulse. The number of excitations n_{S_0} is approximately given by $n_{S_0} = 1 - \exp(-k_{\text{ex}} \tau_{\text{ex}})$, where we neglect spontaneous decays during the pulse according to our assumptions. However, for high excitation rates, the effective excitation rate $k_{\text{ex}}^* = k_{\text{ex}} k_{\text{vib}} / (k_{\text{ex}} + k_{\text{vib}})$ should be used. Furthermore, if the STED pulse overlaps the excitation pulse, the (net) number of excitations is reduced to the dynamic equilibrium of the fluorescence excitation and suppression rates and reaches approximately

$$n_{S_0}^* = \frac{k_{\text{ex}}^*}{k_{\text{ex}}^* + k_{S_1}(1 + \gamma)} \left(1 - \exp(-k_{\text{ex}}^* + k_{S_1}(1 + \gamma)) \tau_{\text{ex}} \right). \quad (12)$$

Validity of the effective STED rate

For the sake of simplicity and physical insight, we solved the rate Eqs. (1) at the dynamic equilibrium and found the effective STED rate $k_{\text{STED}}^* = \gamma k_{\text{S1}} = k_{\text{STED}} k_{\text{vib}} / (k_{\text{STED}} + k_{\text{vib}})$. On the other hand, the exact solution of the time-varying population $P_{\text{S1}}(t)$ reads as

$$P_{\text{S1}}(0 < t < \tau_{\text{STED}}) = \frac{k_{\text{S1}} - k_{\text{vib}} + k_1}{2k_1} \exp\left(-\frac{k_2 + k_1}{2} t\right) - \frac{k_{\text{S1}} - k_{\text{vib}} - k_1}{2k_1} \exp\left(-\frac{k_2 - k_1}{2} t\right), \quad (13)$$

where $k_1 = \sqrt{(k_{\text{vib}} - k_{\text{S1}})^2 + 4k_{\text{STED}}^2}$ and $k_2 = k_{\text{vib}} + k_{\text{S1}} + 2k_{\text{STED}}$. Thereafter, $P_{\text{S1}}(t)$ decays with the rate k_{S1} for the remainder of the pulse period T as outlined before. The integration of $q_{\text{fl}} k_{\text{S1}} P_{\text{S1}}(t)$ for $0 < t < T$ is straightforward and yields the probability of fluorescence $F(\gamma)$, from which we again calculate $\eta_{\text{ps}} = F(\gamma)/F(0)$. Equation (13) can be simplified by noting that $k_{\text{vib}} \pm k_{\text{S1}} \approx k_{\text{vib}}$. However, it is not obvious to get Eq. (3) as the STED rate k_{STED} in the doughnut crest may approach or even surpass k_{vib} , which prohibits any further simplification. Therefore, Fig. 7 compares the exact results with those obtained by Eq. (3) (Fig. 2) showing the excellent agreement at all relevant conditions in the outlined examples. Notable differences occur only at very short STED pulses, at which the condition $\tau_{\text{STED}} \gg 1/k_{\text{vib}}$ is violated and our assumption of a dynamic (pseudo-)equilibrium during the STED pulse fails.

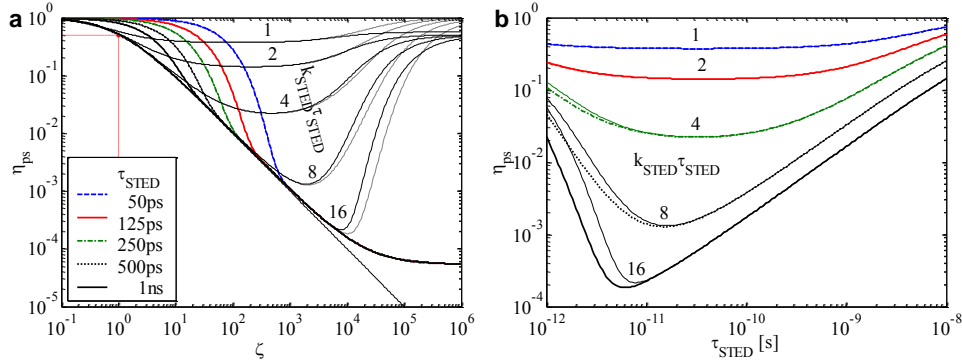


Fig. 7. Probability of spontaneous decay η_{ps} obtained with Eq. (3) compared to the exact results based on Eq. (13) for the very same parameters as described in Fig. 2. The exact results are overlaid as thin lines and are in excellent agreement except at STED pulse widths $\tau_{\text{STED}} < 10\text{ps}$.

Continuous wave excitation

Continuous wave (CW) excitation requires CW STED, which simplifies the calculations because pulse synchronization and timing is not required. The calculation of the spontaneous decay rate k_{CW} and the probability of spontaneous decay η_{CW} are straightforward. Let k_{STED}^* be the effective STED rate $k_{\text{STED}}^* = \gamma k_{\text{S1}} = k_{\text{STED}} k_{\text{vib}} / (k_{\text{STED}} + k_{\text{vib}})$ as defined before, and let $q_{\text{isc}}^* = q_{\text{isc}} k_{\text{S1}} / (k_{\text{S1}} + k_{\text{STED}}^*) = q_{\text{isc}} / (1 + \gamma)$ be the corresponding intersystem crossing yield. At the dynamic equilibrium, the average cycle time τ_{CW} is then given by the sum of the occupation times of the singlet and triplet states.

$$\tau_{\text{CW}} = \frac{1}{k_{\text{ex}}^*} + \frac{1}{k_{\text{S1}} + k_{\text{STED}}^*} + \frac{q_{\text{isc}}^*}{k_{\text{T1}}} = \frac{1}{k_{\text{ex}}^*} + \frac{1}{k_{\text{S1}}(1 + \gamma)} + \frac{q_{\text{isc}}}{k_{\text{T1}}(1 + \gamma)} \quad (14)$$

The second term is the average time $\tau_{S_1}^*$ the molecule spends in the excited state S_1 . Thus, the average population of S_1 becomes $P_{S_1} = \tau_{S_1}^* / \tau_{CW}$ and the spontaneous decay rate is $k_{CW} = k_{S_1} P_{S_1}$. We finally obtain

$$k_{CW} = \left(\frac{1+\gamma}{k_{ex}^*} + \frac{1}{k_{S_1}} + \frac{q_{isc}}{k_{T_1}} \right)^{-1} \quad \text{and} \quad \eta_{CW} = \left(\frac{1}{k_{ex}^*} + \frac{1}{k_{S_1}} + \frac{q_{isc}}{k_{T_1}} \right) k_{CW}. \quad (15)$$

If the triplet state population is small, i.e. $q_{isc}/k_{T_1} \ll 1/k_{S_1}$, $\eta_{CW} \approx (k_{ex}^* + k_{S_1}) / (k_{ex}^* + (1+\gamma)k_{S_1})$; and if in addition the excitation rate is small, i.e. $k_{ex}^* \ll k_{S_1}$, we obtain again $\eta_{CW} \approx 1/(1+\gamma)$ as for the case 4 in Table 1. This convergence at low CW excitation rate can be expected because individual excitations become well separated in time and, therefore, the fluorophores undergo STED as if a pulsed excitation scheme were used.

Acknowledgments

Marcel Leutenegger is a fellow of the Alexander von Humboldt foundation.